BI-TP 2007/07
arXiv:0704.1720

A resummed perturbative estimate for the quarkonium spectral function in hot QCD

M. Laine

Faculty of Physics, University of Bielefeld, D-33501 Bielefeld, Germany

Abstract

By making use of the finite-temperature real-time static potential that was introduced and computed to leading non-trivial order in Hard Thermal Loop resummed perturbation theory in recent work, and solving numerically a Schrödinger-type equation, we estimate the quarkonium (in practice, bottomonium) contribution to the spectral function of the electromagnetic current in hot QCD. The spectral function shows a single resonance peak which becomes wider and then disappears as the temperature is increased beyond 450 MeV or so. This behaviour can be compared with recently attempted lattice reconstructions of the same quantity, based on the "maximum entropy method", which generically show several peaks. We also specify the dependence of our results on the spatial momentum of the electromagnetic current, as well as on the baryon chemical potential characterising the hot QCD plasma.

June 2007

1. Introduction

It was suggested long ago that the properties of heavy quarkonium may be very sensitive to the deconfinement transition that takes place in thermal QCD, in spite of the fact that the deconfinement temperature is much below the heavy quark mass [1]. Consequently, heavy quarkonium has become one of the classic probes for quark-gluon plasma formation in heavy ion collision experiments (for an extensive review, see ref. [2]).

In order to understand the physics involved, let us start by recalling that the way in which the properties of thermally produced heavy quarkonium can be observed, is through its decay into a virtual photon, which then produces a lepton–antilepton pair [3]. Leptons do not feel strong interactions, and escape the thermal system. Measuring their energy spectrum at around $E \simeq 2M$, where M is the heavy quark mass, thus yields first-hand information on the "in-medium" properties of heavy quarkonium.

To appreciate why the in-medium properties of heavy quarkonium can change already just above the deconfinement transition, it is conventional to consider a non-relativistic potential model for determining the thermally modified energy levels of the decaying bound state [4]–[9]. Above the deconfinement transition, the colour-electric field responsible for binding the heavy quark and antiquark together gets Debye-screened. Once the screening is strong enough, the corresponding Schrödinger equation does not possess bound-state solutions any more. It is said that quarkonium "melts" at this point, and the assumption is that the quarkonium resonance peak should consequently disappear from the dilepton production rate.

Strictly speaking, though, just estimating the energy levels from a potential model does not allow to reconstruct the spectral function (which in turn determines the production rate). In fact, stationary levels would correspond to infinitely narrow peaks in the spectral function, irrespective of the value of the binding energy, while the intuitive picture is that a resonance peak should dissolve through becoming gradually wider. To conform with this expectation, a non-zero width could of course be inserted by hand, as an additional model ingredient. However, this would take us further away from a first principles QCD prediction.

It appears that once the computation is formulated within thermal field theory, there is no need to insert anything by hand. Indeed, it has been pointed out recently that by defining a static potential through a Schrödinger equation satisfied by a certain heavy quarkonium Green's function, and computing it systematically in the weak-coupling expansion (which necessitates Hard Thermal Loop resummation), the static potential obtains both a standard Debye-screened real part, as well as an imaginary part, originating from the Landau-damping of almost static colour fields [10]. The imaginary part of the static potential then leads to a finite width for the quarkonium resonance peak in the spectral function.

In ref. [10], the consequences deriving from the existence of an imaginary part were addressed only semi-quantitatively. It is the purpose of the present note to solve explicitly for the spectral function that the static potential computed in ref. [10] leads to. We also compare qualitatively with attempted lattice reconstructions of the same quantity.

The note is organised as follows. We review the form of the spectral function in the non-interacting limit in Sec. 2. Some properties of the static potential derived in ref. [10] are discussed in Sec. 3. The relevant (time-dependent) Schrödinger equation is set up in Sec. 4, and solved numerically in Sec. 5. We conclude and compare with literature in Sec. 6.

2. Spectral function in the non-interacting limit

We will consider two related correlators in this paper:

$$\tilde{C}_{>}(q^0) \equiv \int_{-\infty}^{\infty} \mathrm{d}t \int \mathrm{d}^3\mathbf{x}\, e^{iQ\cdot x} \Big\langle \hat{\mathcal{J}}^\mu(x) \hat{\mathcal{J}}_\mu(0) \Big\rangle \;, \tag{2.1}$$

where $\hat{\mathcal{J}}^\mu(x) \equiv \hat{\bar{\psi}}(x)\gamma^\mu\hat{\psi}(x)$ is the contribution from a single heavy flavour to the electromagnetic current in the Heisenberg picture (the electromagnetic coupling constant and charge have been omitted for simplicity, and the metric is assumed to be $(+---)$); as well as the spectral function

$$\rho(q^0) \equiv \frac{1}{2}\Big(1 - e^{-\beta q^0}\Big) \tilde{C}_{>}(q^0) \;, \tag{2.2}$$

where $\beta \equiv 1/T$, and T is the temperature. The dilepton production rate is directly proportional to the spectral function [3]. The expectation value in Eq. (2.1) refers to $\langle ... \rangle \equiv \mathcal{Z}^{-1}\mathrm{Tr}\,[\exp(-\hat{H}/T)(...)]$, where $\mathcal{Z}$ is the partition function, and $\hat{H}$ is the QCD Hamiltonian operator. We have assumed a notation where the dependence on the spatial momentum $\mathbf{q}$ is suppressed. A correlator without tilde refers to the situation before taking the Fourier transform with respect to time:

$$C_{>}(t) \equiv \int \mathrm{d}^3\mathbf{x}\, e^{-i\mathbf{q}\cdot\mathbf{x}} \Big\langle \hat{\mathcal{J}}^\mu(t,\mathbf{x}) \hat{\mathcal{J}}_\mu(0,\mathbf{0}) \Big\rangle \;. \tag{2.3}$$

We start by discussing the form of $\rho(q^0)$ in the free theory. Denoting the heavy quark mass by M, we concentrate on frequencies around the two-particle threshold,

$$\omega \equiv q^0 \simeq \sqrt{4M^2 + \mathbf{q}^2} \;, \tag{2.4}$$

and will also assume the spatial momentum $\mathbf{q}$ to be small, $q \equiv |\mathbf{q}| \ll M$.

2.1. Non-relativistic low-temperature regime in full QCD

The free quarkonium contribution to the spectral function of the electromagnetic current can be extracted, for instance, from refs. [11, 12, 9]. Modifications brought in by various lattice discretizations have also been addressed [11, 12, 13]. Here we generalise the continuum expression slightly by including a non-zero quark chemical potential, μ. Restricting first to the case $\mathbf{q} = \mathbf{0}$, the result is very simple:

$$\rho(\omega) \overset{\omega \gtrsim M}{=} -\frac{N_\mathrm{c}}{4\pi} M^2 \theta(\hat{\omega} - 2)\Big(1 - \frac{4}{\hat{\omega}^2}\Big)^{\frac{1}{2}} \Big(\hat{\omega}^2 + 2\Big)\Big[1 - n_\mathrm{F}\Big(\frac{\omega}{2} + \mu\Big) - n_\mathrm{F}\Big(\frac{\omega}{2} - \mu\Big)\Big] \;, \tag{2.5}$$

where $N_c = 3$, n_F is the Fermi distribution function, and we have denoted

$$\hat{\omega} \equiv \frac{\omega}{M} \; . \tag{2.6}$$

Let us now concentrate on the case of low temperatures, $T/(M \pm \mu) \ll 1$ (parametrically, we are interested in temperatures $T \sim g^2 M$ [10]). Then the Fermi distribution functions in Eq. (2.5) are exponentially small. We thus find immediately that the spectral function is independent of μ in this limit.

Restricting furthermore to the non-relativistic regime, $|\hat{\omega} - 2| \ll 1$, and considering the external momentum q to be small, $q \ll M$, it is easy to include dependence on q. We obtain

$$\rho(\omega) \overset{\omega \simeq 2M}{=} -\frac{3N_c M^2}{2\pi} \theta\Big(\hat{\omega} - 2 - \frac{q^2}{4M^2}\Big)\Big(\hat{\omega} - 2 - \frac{q^2}{4M^2}\Big)^{\frac{1}{2}} \left[1 + \mathcal{O}\Big(\hat{\omega} - 2 - \frac{q^2}{4M^2}, \frac{q^2}{M^2}\Big)\right] . \tag{2.7}$$

2.2. Representation through a Schrödinger equation

We next demonstrate that the result of Eq. (2.7) can be reproduced by a certain Schrödinger equation. The Schrödinger equation requires the introduction of an intermediate point-splitting vector $\mathbf{r}$ which will be set to zero at the end of the computation. The relevant equation reads (cf. Eq. (2.4) of ref. [10])

$$\left[i\partial_t - \left(2M - \frac{\nabla_{\mathbf{r}}^2}{M}\right)\right]\check{C}_>(t, \mathbf{r}) = 0 \; , \tag{2.8}$$

with the initial condition

$$\check{C}_>(0, \mathbf{r}) = -6N_c \, \delta^{(3)}(\mathbf{r}) \; . \tag{2.9}$$

In Eq. (2.8) we have set for simplicity $\mathbf{q} = \mathbf{0}$, but the center-of-mass kinetic energy $q^2/4M$ can be trivially added to the rest mass $2M$. After having solved the equation, the function in Eq. (2.3) is obtained through

$$C_>(t) \equiv \check{C}_>(t, \mathbf{0}) \; . \tag{2.10}$$

We search for a solution of Eq. (2.8) with the ansatz

$$\check{C}_>(t, \mathbf{r}) \equiv \int \frac{\mathrm{d}^4 P}{(2\pi)^4} e^{-ip_0 t + i\mathbf{p}\cdot\mathbf{r}} \mathcal{F}(p_0, \mathbf{p}) \; . \tag{2.11}$$

Eq. (2.8) dictates that

$$p_0 = 2M + \frac{\mathbf{p}^2}{M} \equiv E_{\mathbf{p}} \; , \tag{2.12}$$

leading to the modified ansatz

$$\check{C}_>(t, \mathbf{r}) \equiv \int \frac{\mathrm{d}^3 \mathbf{p}}{(2\pi)^3} e^{-iE_{\mathbf{p}} t + i\mathbf{p}\cdot\mathbf{r}} \mathcal{F}(\mathbf{p}) \; . \tag{2.13}$$

The initial condition in Eq. (2.9) can be satisfied provided that $\mathcal{F}(\mathbf{p}) = -6N_\mathrm{c}$. The point-splitting can now be trivially removed, cf. Eq. (2.10), and a Fourier-transform finally yields

$$\begin{aligned}\tilde{C}_>(\omega) &= \int_{-\infty}^{\infty} \mathrm{d}t\, e^{i\omega t} \check{C}_>(t,\mathbf{0}) \\ &= -12\pi N_\mathrm{c} \int \frac{\mathrm{d}^3\mathbf{p}}{(2\pi)^3}\, \delta\Big(\omega - 2M - \frac{\mathbf{p}^2}{M}\Big) \\ &= -\frac{3N_\mathrm{c}M^2}{\pi} \theta(\hat\omega - 2)(\hat\omega - 2)^{\frac{1}{2}} \;, \end{aligned} \tag{2.14}$$

where we have used the dimensionless variable in Eq. (2.6). The spectral function is given by Eq. (2.2); since we are in the non-relativistic limit $|\hat\omega - 2| \ll 1$ and at low temperatures $T \ll M$, the factor $\exp(-\beta\omega) \sim \exp(-2M/T)$ can be neglected, whereby $\rho(\omega) = \tilde{C}_>(\omega)/2$. Replacing furthermore $2M \to 2M + q^2/4M$, yields then directly Eq. (2.7), as promised.

3. Real-time static potential

In order to account for interactions, a static potential can be inserted into the Schrödinger equation. The appropriate object, denoted by $V^{(2)}_>(t,r)$, was defined and computed to leading non-trivial order in Hard Thermal Loop resummed perturbation in ref. [10] (cf. Eq. (3.17)). Reorganizing the result in a way where the symmetry of the integrand under $p^0 \leftrightarrow -p^0$ is explicit, we rewrite it as

$$V^{(2)}_>(t,r) = -\frac{g^2C_F}{4\pi}\bigg[m_\mathrm{D} + \frac{\exp(-m_\mathrm{D}r)}{r}\bigg] + \delta V^{(2)}_>(t,r) \;, \tag{3.1}$$

$$\begin{aligned}\delta V^{(2)}_>(t,r) &= g^2C_F \int \frac{\mathrm{d}^3\mathbf{p}}{(2\pi)^3} \frac{2 - e^{ip_3r} - e^{-ip_3r}}{2} \times \\ &\times \bigg\{ \int_{-\infty}^{\infty} \frac{\mathrm{d}p^0}{\pi} p^0 \Big[e^{-i|p^0|t} + n_\mathrm{B}(|p^0|)\Big(e^{-i|p^0|t} - e^{i|p^0|t}\Big)\Big] \times \\ &\times \bigg[\Big(\frac{1}{\mathbf{p}^2} - \frac{1}{(p^0)^2}\Big)\rho_E(p^0,\mathbf{p}) + \Big(\frac{1}{p_3^2} - \frac{1}{\mathbf{p}^2}\Big)\rho_T(p^0,\mathbf{p})\bigg]\bigg\} \;. \end{aligned} \tag{3.2}$$

Here $C_F \equiv (N_\mathrm{c}^2 - 1)/2N_\mathrm{c}$, m_D is the Debye mass parameter, and we have chosen $\mathbf{r} \equiv (0,0,r)$. The r-independent term in Eq. (3.1) amounts to twice a thermal mass correction for the heavy quark. The functions ρ_E, ρ_T are specified in Appendix A. The Schrödinger equation to be solved reads

$$\bigg[i\partial_t - \bigg(2M - \frac{\nabla_\mathbf{r}^2}{M} + V^{(2)}_>(t,r)\bigg)\bigg]\check{C}_>(t,\mathbf{r}) = 0 \;, \tag{3.3}$$

with the initial condition in Eq. (2.9), and the replacement $2M \to 2M + q^2/4M$ for $q \neq 0$.

3.1. Dynamical scales

Let us review the time and distance scales that play a role in the solution of Eq. (3.3). The derivatives in the free part must be of similar magnitudes (after trivially shifting away the

constant $2M$), implying that

$$\frac{1}{t} \sim \left(\frac{1}{r}\right)^2 \frac{1}{M} \; . \tag{3.4}$$

At the same time, they must also be of similar magnitude as the potential. Given that the potential is screened, this means

$$\left(\frac{1}{r}\right)^2 \frac{1}{M} \lesssim \frac{g^2}{r} \quad \Leftrightarrow \quad \frac{1}{r} \lesssim g^2 M \; . \tag{3.5}$$

Therefore, we obtain

$$\frac{1}{t} \lesssim g^2 \frac{1}{r} \; , \tag{3.6}$$

i.e. the time scales relevant for the solution around the resonance peak are much larger than the spatial distance scales. Consequently, in order to obtain a formally consistent approximation to a fixed order in g, we need to take the limit $t \gg r$ in the static potential.

Even though it has thus become clear that only the limit $t \gg r$ of the potential is needed at the first non-trivial order in g^2, we nevertheless discuss in the remainder of this section how the infinite-time limit is approached, perhaps learning on the way something about the convergence of the weak-coupling expansion.

3.2. Zero-temperature part

Let us first compute $\delta V^{(2)}_{>}(t,r)$ in the zero-temperature limit. In this case $n_{\rm B}(|p^0|) \to 0$ and

$$\rho_E(p^0,\mathbf{p}) = \rho_T(p^0,\mathbf{p}) = \pi\, \mathrm{sign}(p^0)\delta((p^0)^2 - \mathbf{p}^2) \; . \tag{3.7}$$

Given that the prefactor in front of ρ_E vanishes on-shell, ρ_E does not contribute in this limit, and we simply obtain

$$\delta V^{(2)}_{>}(t,r) = g^2 C_F \int \frac{\mathrm{d}^3\mathbf{p}}{(2\pi)^3} \frac{2 - e^{ip_3 r} - e^{-ip_3 r}}{2} e^{-ipt} \left(\frac{1}{p_3^2} - \frac{1}{p^2} \right) , \tag{3.8}$$

where $p \equiv |\mathbf{p}|$. Even though it is obvious that this contribution vanishes for $t \to \infty$, its precise evaluation requires the introduction of an intermediate regulator, because the absolute value of the p-integrand grows linearly with p. We can either set $t \to t - i\epsilon$, with $\epsilon \to 0^+$ at the end of the computation, or regulate the spatial integration by going to $d = 3 - 2\epsilon$ dimensions. In the first case the integral can be rewritten as

$$\delta V^{(2)}_{>}(t,r) = \frac{g^2 C_F}{(2\pi)^2} \int_{-1}^{1} \mathrm{d}z \left(\frac{1}{z^2} - 1 \right) \int_0^\infty \mathrm{d}p\, e^{-p\epsilon} \Big[e^{-ipt} - e^{ip(rz - t)} \Big] \; ; \tag{3.9}$$

in the latter case the "convergence factor" $e^{-p\epsilon}$ is replaced by $p^{-2\epsilon}$. Either way, the p-integral can be carried out (in the former case, $\int_0^\infty \mathrm{d}p\, e^{-p\epsilon} e^{-ipx} = 1/(ix + \epsilon)$; in the latter

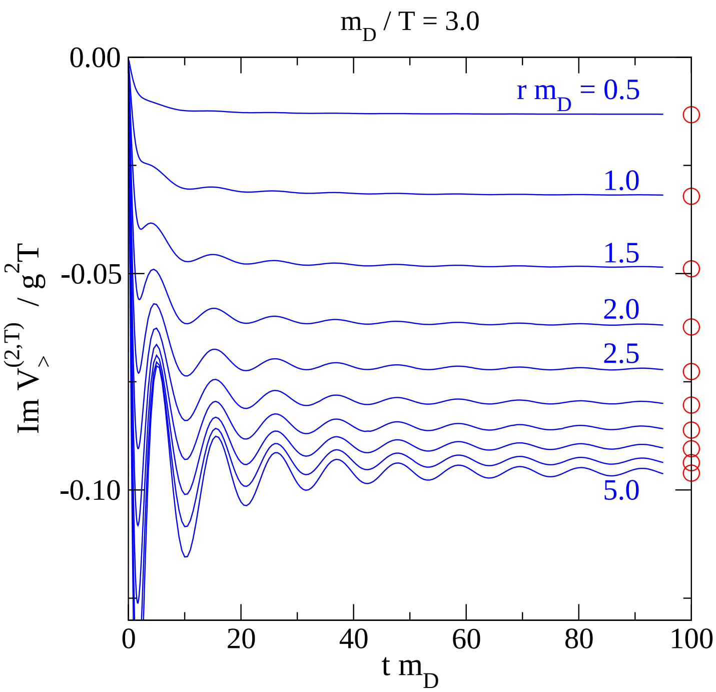

Figure 1: The part of $\delta V_>^{(2)}(t,r)$ that remains finite for $t\to\infty$ (cf. Sec. 3.3). The circles at right denote the asymptotic values in this limit. The oscillations visible at large rm_D have the frequency $\omega_\mathrm{pl} = m_\mathrm{D}/\sqrt{3}$; the corresponding oscillation period in terms of the variable tm_D is $2\pi\sqrt{3}\approx 10.9$.

case, $\int_0^\infty \mathrm{d}p\, p^{-2\epsilon} e^{-ipx} = \Gamma(1-2\epsilon)/(ix)^{1-2\epsilon}$), and subsequently, also the z-integral (as long as we stay within the light cone). We obtain, for $t>r$,

$$\delta V_>^{(2)}(t,r) \;=\; g^2 C_F \frac{i}{4\pi^2 t}\biggl[2+\frac{r}{t}\biggl(1-\frac{t^2}{r^2}\biggr)\ln\frac{t+r}{t-r}\biggr] \approx g^2 C_F \frac{ir^2}{3\pi^2 t^3}\;, \quad \text{for } t\gg r\;. \tag{3.10}$$

The result is, thus, purely imaginary, and vanishes rapidly with time. For $t^{-1}\sim g^2 r^{-1}$, it corresponds parametrically to an effect of order $\mathcal{O}(g^8/r)$, and should be neglected.

3.3. Finite-temperature part

Considering then $\delta V_>^{(2)}(t,r)$ at finite temperatures, there are two different types of new structures emerging. First of all, there is the term without $n_\mathrm{B}(|p^0|)$ in Eq. (3.2). This amounts to a generalization of the potential in Sec. 3.2 through the introduction of one new dimensionful parameter, m_D, appearing in the spectral functions. Second, there is the term with $n_\mathrm{B}(|p^0|)$. This introduces a further new dimensionful parameter, T, and complicates the functional dependence further.

The evaluation of the term without $n_\mathrm{B}(|p^0|)$ again requires the introduction of a regulator, as in Sec. 3.2. The resulting potential has both a real and an imaginary part. However, it still decays fast for $t\gg r$; the only difference with respect to Sec. 3.2 is that the decay is not

purely powerlike any more, but the existence of a new scale leads to oscillations as well. In particular, at large r the behaviour is dominated by small p, and then the oscillations take place with the familiar plasmon frequency, $\omega_{\rm pl} = m_{\rm D}/\sqrt{3}$ (cf. Eqs. (A.11), (A.12)).

On the other hand, the term with $n_{\rm B}(|p^0|)$ leads to more dramatic new effects. As is obvious from Eq. (3.2), the contribution from this term to the static potential is purely imaginary. Also, this part can be evaluated without regularization, since $n_{\rm B}(|p^0|)$ makes the p-integral rapidly convergent (assuming that the p^0-integral is carried out first). On the contrary, $n_{\rm B}(|p^0|)$ modifies the large-t behaviour of $\delta V^{(2)}_{>}(t,r)$ significantly, since it is Bose-enhanced, $n_{\rm B}(|p^0|) \approx T/|p^0|$, for $|p^0| \ll T$. In fact, the contribution from this term does not vanish for $t \to \infty$, but leads to a finite imaginary part for $\delta V^{(2)}_{>}(\infty,r)$ [10].

In order to illustrate this behaviour, let us evaluate the term with $n_{\rm B}(|p^0|)$ numerically. An example is shown in Fig. 1. We indeed observe that the imaginary part of the potential approaches a finite value at large t.

4. Solution of the Schrödinger equation

As argued in the previous section, the static potential in Eq. (3.3) should be evaluated in the limit $t \gg r$, yielding in dimensional regularization (cf. Eqs. (4.3), (4.4) of ref. [10])

$$\lim_{t\to\infty} V^{(2)}_{>}(t,r) \quad = \quad -\frac{g^2 C_F}{4\pi}\left[m_{\rm D} + \frac{\exp(-m_{\rm D} r)}{r}\right] - \frac{i g^2 T C_F}{4\pi}\,\phi(m_{\rm D} r)\;, \tag{4.1}$$

where the function

$$\phi(x) \equiv 2\int_0^\infty \frac{{\rm d}z\, z}{(z^2+1)^2}\left[1 - \frac{\sin(zx)}{zx}\right] \tag{4.2}$$

is finite and strictly increasing, with the limiting values $\phi(0) = 0$, $\phi(\infty) = 1$.

Before proceeding, it is appropriate to point out that by solving Eq. (3.3) we only account for a part of the $\mathcal{O}(g^2)$-corrections, namely those which are temperature-dependent and change the t-dependence (or, after the Fourier-transform, the ω-dependence) of the solution. Apart from these corrections, there are also other corrections, well-known from zero-temperature computations. In particular, the precise meaning of the mass parameter M should be specified; a matching computation between QCD and NRQCD [14] shows that it actually corresponds to a quark pole mass, whose relation to the commonly used $\overline{\rm MS}$ mass is known up to 3-loop order [15]. Furthermore, the “normalization” of the NRQCD-representative of the electromagnetic current can be worked out by another matching computation: this relation is known up to 2-loop level [16]. In our language, this amounts to a radiative correction to the initial condition in Eq. (2.9). Neither of these zero-temperature corrections plays an essential role for the thermal effects that we are interested in here, and consequently both will be ignored in the following.

4.1. General procedure

Now, once Eq. (3.3) has been solved, we can extrapolate $\mathbf{r} \to \mathbf{0}$, to obtain $C_>(t) = \check{C}_>(t,\mathbf{0})$. Symmetries indicate that $C_>(-t) = C^*_>(t)$, whereby the Fourier transform from $C_>(t)$ to $\tilde{C}_>(\omega)$ can be written as an integral over the positive half-axis. Recalling finally the relation of $\tilde{C}_>(\omega)$ and the spectral function, Eq. (2.2), we can write the latter as

$$\rho(\omega) = \Big(1 - e^{-\beta\omega}\Big) \int_0^\infty \mathrm{d}t \,\Big\{\cos(\omega t)\,\mathrm{Re}\Big[\check{C}_>(t,\mathbf{0})\Big] - \sin(\omega t)\,\mathrm{Im}\Big[\check{C}_>(t,\mathbf{0})\Big]\Big\} \,. \tag{4.3}$$

Concentrating on the non-relativistic regime, i.e. on frequencies close to the quarkonium mass, we write

$$\omega \equiv 2M + \omega' \,, \tag{4.4}$$

with $|\omega'| \ll M$. It is also convenient to introduce

$$\check{C}_>(t,\mathbf{r}) \equiv e^{-i2Mt}\,\frac{u(t,\mathbf{r})}{r} \,. \tag{4.5}$$

Finally, we assume the point-split solution to be spherically symmetric (S-wave); in the following we denote it by $u(t,r)$. Thereby Eq. (4.3) becomes

$$\rho(\omega) = \Big[1 - e^{-\beta(2M+\omega')}\Big] \int_0^\infty \mathrm{d}t \,\Big\{\cos(\omega' t)\,\mathrm{Re}\Big[\psi(t,0)\Big] - \sin(\omega' t)\,\mathrm{Im}\Big[\psi(t,0)\Big]\Big\} \,, \tag{4.6}$$

where

$$\psi(t,0) \equiv \lim_{r\to 0} \frac{u(t,r)}{r} \,, \tag{4.7}$$

and the Schrödinger equation reads

$$i\partial_t u(t,r) = \Big[-\frac{1}{M}\frac{\mathrm{d}^2}{\mathrm{d}r^2} + V^{(2)}_>(\infty,r)\Big] u(t,r) \,, \tag{4.8}$$

with the initial condition

$$u(0,r) = -6N_\mathrm{c}\, r\delta^{(3)}(\mathbf{r}) \,, \tag{4.9}$$

and the boundary condition

$$u(t,0) = 0 \,. \tag{4.10}$$

We note that the prefactor in Eq. (4.6) can be set to unity, since we are in any case omitting exponentially small contributions $\sim \exp(-2M/T)$.

4.2. Discretised system

In order to solve Eq. (4.8) numerically, we discretise both the spatial coordinate r and the time coordinate t.[1] We denote the spatial lattice spacing by a_s and the temporal one by a_t.

[1] Let us stress that this discretization is related to the solution of a classical partial differential equation; it has nothing to do with the regularization used in QCD. Indeed, Eq. (4.1) assumes the use of dimensional regularization on the QCD side.

Furthermore, $r_{\max}$ and $t_{\max}$ are the maximal values of these coordinates; there are $N_s + 1$ spatial sites, and $N_t + 1$ temporal sites, with $r_{\max} = N_s a_s$, $t_{\max} = N_t a_t$.

Let us start by discussing the discretization of the initial condition in Eq. (4.9). In continuum, we can formally write

$$
\begin{aligned}
r\delta^{(3)}(\mathbf{r}) &= r\int \frac{\mathrm{d}^3\mathbf{p}}{(2\pi)^3}\, e^{i\mathbf{p}\cdot\mathbf{r}} = \frac{r}{4\pi^2}\int_0^\infty \mathrm{d}p\, p^2 \int_{-1}^{+1} \mathrm{d}z\, e^{iprz} \\
&= \frac{1}{4\pi^2 i}\int_{-\infty}^{\infty} \mathrm{d}p\, p\, e^{ipr} \; .
\end{aligned}
\tag{4.11}
$$

On the lattice, with $r = na_s$, $n = 0, 1, ..., N_s$, a possible discretization of Eq. (4.11), possessing formally the correct continuum limit at $a_s \to 0$, is given by

$$
\begin{aligned}
r\delta^{(3)}(\mathbf{r}) &\to \frac{1}{4\pi^2 i}\int_{-\pi/a_s}^{\pi/a_s} \mathrm{d}p\, \frac{2}{a_s}\sin\Big(\frac{a_s p}{2}\Big) e^{ipna_s} \\
&= \Big(\frac{2}{\pi a_s}\Big)^2 \frac{n}{4n^2-1}(-1)^{n+1} \; .
\end{aligned}
\tag{4.12}
$$

We will see in Sec. 4.3 from another angle that Eq. (4.12) indeed provides for a correct and very convenient discretization of the initial condition (once multiplied by $-6N_\mathrm{c}$).

As far as the spatial derivative in Eq. (4.8) is concerned, we discretise it in the usual way:

$$
\frac{\mathrm{d}^2 u(t,r)}{\mathrm{d}r^2} \to \frac{u(t,(n-1)a_s) - 2u(t,na_s) + u(t,(n+1)a_s)}{a_s^2} \; , \quad n = 1, 2, ..., N_s - 1 \; , \tag{4.13}
$$

with the boundary condition in Eq. (4.10). Furthermore we also set the boundary condition

$$
u(t, N_s a_s) \equiv 0 \; , \tag{4.14}
$$

whose justification requires that we check the independence of the results on N_s (or $r_{\max}$).

As far as the discretization of the time derivative is concerned, the general issues arising are well described in §19.2 of ref. [17]. Writing Eq. (4.8) in the form

$$
i\partial_t u = \hat{H} u \; , \tag{4.15}
$$

we use the "Crank-Nicolson method", which amounts to solving

$$
\Big(1 + \frac{1}{2}\, i\hat{H} a_t\Big) u(t + a_t, r) = \Big(1 - \frac{1}{2}\, i\hat{H} a_t\Big) u(t, r) \; . \tag{4.16}
$$

This method leads to an evolution which is accurate up to $\mathcal{O}(a_t^2)$, stable, and unitary (the last one provided that $\hat{H}$ were hermitean, which is not the case in our study).

Given the solution for $u(t, na_s)$, we then extrapolate for $\psi(t, 0)$ (cf. Eq. (4.7)) simply through

$$
\psi(t, 0) \equiv \frac{u(t, a_s)}{a_s} \; . \tag{4.17}
$$

4.3. Non-interacting limit in the discretised system

The spectral function following from the discretization of Sec. 4.2, after the result has been inserted into Eq. (4.6), can be found analytically in the free theory, if we take the limits $a_t/a_s \to 0$, $r_{\rm max}, t_{\rm max} \to \infty$. The solution is quite illuminating, so we briefly discuss it here.

Let us start by introducing the notation

$$\tilde{p} \equiv \frac{2}{a_s}\sin\Big(\frac{a_s p}{2}\Big) \;, \quad \mathring{p} \equiv \frac{1}{a_s}\sin(a_s p) \;. \tag{4.18}$$

Then a general solution of Eq. (4.8) [without $V^{(2)}_{>}(\infty, r)$ and with the spatial derivative replaced by Eq. (4.13)] can be written as

$$u(t,r) = \int_{-\pi/a_s}^{\pi/a_s} \frac{{\rm d}p}{2\pi}\, e^{-i\tilde{p}^2 t/M + ipr} \mathcal{F}(p) \;. \tag{4.19}$$

Satisfying the initial condition in Eqs. (4.9), (4.12) requires

$$\mathcal{F}(p) = -6N_{\rm c}\frac{\tilde{p}}{2\pi i} \;. \tag{4.20}$$

Furthermore, extracting the function $\psi(t,0)$ according to Eq. (4.17) yields

$$\psi(t,0) = -6N_{\rm c}\frac{1}{4\pi^2}\int_{-\pi/a_s}^{\pi/a_s} {\rm d}p\, \tilde{p}\, \mathring{p}\, e^{-i\tilde{p}^2 t/M} \;, \tag{4.21}$$

the Fourier-transform of which reads (cf. Eq. (4.6) in the limit $\exp[-(2M+\omega')/T] = 0$)

$$\begin{aligned} \rho(\omega) &= -\frac{3N_{\rm c}}{2\pi}\int_{-\pi/a_s}^{\pi/a_s} {\rm d}p\, \tilde{p}\, \mathring{p}\, \delta\Big(\omega' - \frac{\tilde{p}^2}{M}\Big) \\ &= -\frac{6N_{\rm c}}{\pi a_s^2}\int_0^\pi {\rm d}x\, \sin(x)\sin\Big(\frac{x}{2}\Big)\delta\Big(a_s\omega' - \frac{4\sin^2(x/2)}{a_s M}\Big) \;, \end{aligned} \tag{4.22}$$

where $\omega' = \omega - 2M$. This integral can be carried out, with the outcome

$$\rho(\omega) = -\frac{3N_{\rm c}M^2}{2\pi}\,\theta(\hat{\omega}-2)\,\theta\Big(\frac{4}{a_s^2M^2} + 2 - \hat{\omega}\Big)\Big(\hat{\omega}-2\Big)^{\frac{1}{2}} \;. \tag{4.23}$$

We note that Eq. (4.23) agrees exactly with Eq. (2.7), except that it is cut off sharply at $(\hat{\omega}-2)_{\rm max} = (2/a_s M)^2$. For addressing the non-relativistic regime $|\hat{\omega}-2| \ll 1$ it is then sufficient to choose $a_s \le 2/M$ for first estimates; at the end, one of course has to extrapolate $a_s \to 0$.

5. Numerical results

In a practical solution, we are not in the limit $a_t/a_s \to 0$ as in Sec. 4.3, but a_t is finite, and $t_{\rm max}, r_{\rm max}$ are finite as well. Then the time variable takes values $t = na_t$, $n = 0, ..., N_t$,

while frequencies assume the values $\omega = \pi m / t_{\rm max}$, $m = -N_t, ..., N_t$. The Fourier-integral in Eq. (4.6) is replaced by a discrete sum; to keep discretization errors at $\mathcal{O}(a_t^2)$, we write it as

$$\int_0^{t_{\rm max}} {\rm d}t\, \mathcal{F}(t) \to \frac{1}{2}\, a_t \biggl[\sum_{n=0}^{N_t - 1} \mathcal{F}(n a_t) + \sum_{n=1}^{N_t} \mathcal{F}(n a_t) \biggr] \;. \tag{5.1}$$

For the parameter values needed we employ simple analytic expressions that can be extracted from Ref. [18],

$$g^2 \simeq \frac{8\pi^2}{9 \ln(9.082\, T / \Lambda_{\overline{\rm MS}})} \;, \quad m_{\rm D}^2 \simeq \frac{4\pi^2 T^2}{3 \ln(7.547\, T / \Lambda_{\overline{\rm MS}})} \;, \qquad \text{for } N_{\rm c} = N_{\rm f} = 3 \;. \tag{5.2}$$

We fix $\Lambda_{\overline{\rm MS}} \simeq 300$ MeV; the width we will find does not depend significantly on this (see also Fig. 2 of ref. [10]). For the mass we insert the bottom quark mass, $M \simeq 4.25$ GeV. We denote the "Bohr radius" by

$$r_B \equiv \frac{8\pi}{g^2 C_F M} \;. \tag{5.3}$$

In the range of temperatures considered, $g^2 C_F / (4\pi) \sim 0.5...0.3$, and $r_B \sim (4...6)/M$.

As typical values of the numerics-related parameters, we have used $r_{\rm max} = 120\, r_B$, $t_{\rm max} = r_{\rm max}$, $a_t = a_s/5$. The dependence on all of these parameters is beyond the visual resolution. By contrast, there is significant dependence on a_s, given that discretization errors are only of order $\mathcal{O}(a_s)$. We have consequently used several values and carried out a linear extrapolation to $a_s \to 0$. A sufficient precision can be obtained, for instance, by using the values $a_s = r_B/12$ and $a_s = r_B/24$ for the extrapolation.

The final result of our analysis is shown in Fig. 2. The curve "500 MeV $\ll T \ll M$" refers to the non-interacting result in Eq. (2.7).

6. Conclusions

The purpose of this note has been to present a numerical estimate for the heavy quarkonium contribution to the spectral function of the electromagnetic current, based on Eqs. (2.9), (3.3), (4.1). The conceptually new ingredient here is the inclusion of a thermal width through the imaginary part of the static potential in Eq. (4.1).

The result we find, Fig. 2, shows a clear resonance peak which rapidly dissolves as the temperature is increased. Even though we do not expect the precise position and height of the peak to be quantitatively accurate, since higher-order perturbative corrections can be large in the temperature range considered (certainly up to 20%), it is comforting that a phenomenologically reasonable pattern arises from such a simple-minded computation.

The result shown in Fig. 2 assumes that the spatial momentum of the electromagnetic current vanishes, $q = 0$. However, as discussed in Sec. 2.1, a non-zero q simply shifts the patterns horizontally by the center-of-mass energy $q^2/4M$ of the heavy quark–antiquark pair,

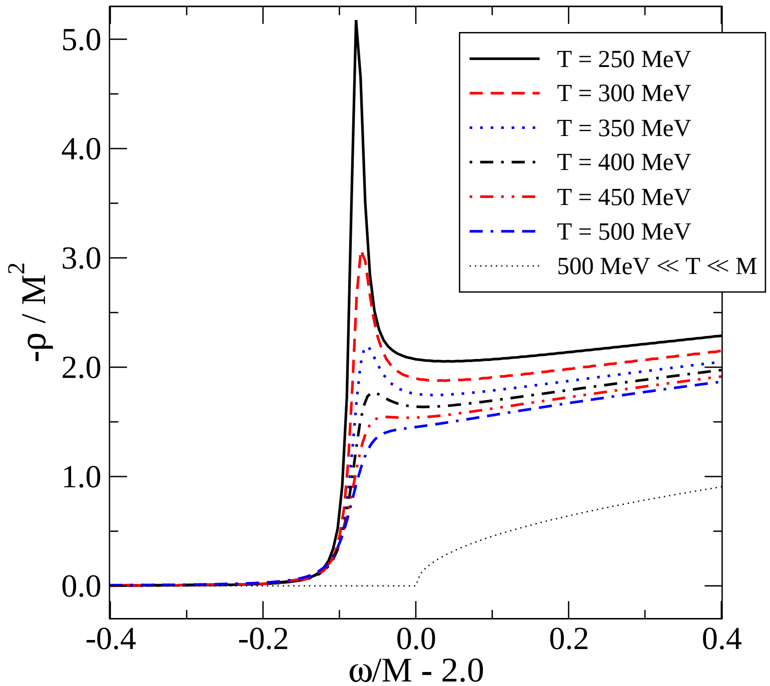

Figure 2: The bottomonium contribution to the spectral function of the electromagnetic current, divided by $-M^2$, in the non-relativistic regime $|\omega/M - 2| \ll 1$.

provided that $q \ll M$. Furthermore, as also pointed out in Sec. 2.1, the dependence on the quark chemical potential μ is exponentially small in the range $(M \pm \mu)/T \gg 1$.

There has been a fair amount of interest in estimating the quarkonium spectral function from lattice QCD, mostly by making use of the so-called maximum entropy method [19]–[24]. Generically, these results show several resonance peaks, rather than just one as in Fig. 2. It has been suspected that the additional peaks may in fact be lattice artefacts. In spite of its own uncertainties, our computation seems to support such an interpretation. As far as the first peak is concerned, systematic uncertainties and different parametric choices do not allow for a quantitative comparison at the present time, but the patterns found on the lattice and in our study do appear to bear at least some qualitative resemblance to each other.

Acknowledgements

I wish to thank O. Philipsen, P. Romatschke and M. Tassler for useful discussions. This work was partly supported by the BMBF project *Hot Nuclear Matter from Heavy Ion Collisions and its Understanding from QCD*.

Appendix A. Auxiliary functions for Eq. (3.2)

For completeness, we specify here the gluonic spectral functions that appear in Eq. (3.2). In order to compactify the expressions somewhat, we introduce the notation

$$y \equiv \frac{p^0}{|\mathbf{p}|} \;, \quad p \equiv |\mathbf{p}| \;. \tag{A.1}$$

Then ρ_T, ρ_E (cf. Appendix B of ref. [10] and references therein) can be written as

$$\begin{aligned}
\rho_T(p^0,\mathbf{p}) &= \theta(y^2-1)\pi\,\mathrm{sign}(y)\delta(\Delta_T(y,p)) + \frac{\theta(1-y^2)\Gamma_T(y,p)}{\Delta_T^2(y,p)+\Gamma_T^2(y,p)} \;, && \text{(A.2)}\\
\Delta_T(y,p) &\equiv p^2(y^2-1) - \frac{m_\mathrm{D}^2}{2}\biggl[y^2 + \frac{y}{2}\Bigl(1-y^2\Bigr)\ln\Bigl|\frac{y+1}{y-1}\Bigr|\biggr] \;, && \text{(A.3)}\\
\Gamma_T(y,p) &\equiv \frac{\pi m_\mathrm{D}^2}{4} y\Bigl(1-y^2\Bigr) \;, && \text{(A.4)}\\
(y^2-1)\rho_E(p^0,\mathbf{p}) &= \theta(y^2-1)\pi\,\mathrm{sign}(y)\delta(\Delta_E(y,p)) + \frac{\theta(1-y^2)\Gamma_E(y,p)}{\Delta_E^2(y,p)+\Gamma_E^2(y,p)} \;, && \text{(A.5)}\\
\Delta_E(y,p) &\equiv p^2 + m_\mathrm{D}^2\biggl[1 - \frac{y}{2}\ln\Bigl|\frac{y+1}{y-1}\Bigr|\biggr] \;, && \text{(A.6)}\\
\Gamma_E(y,p) &\equiv \frac{\pi m_\mathrm{D}^2}{2} y \;. && \text{(A.7)}
\end{aligned}$$

It can be seen that there is in each case a contribution from the "plasmon" pole, as well as from the cut representing Landau damping. Restricting the integration to $p^0 > 0$ thanks to reflection symmetry, the plasmon poles trivially yield

$$\int_1^\infty \mathrm{d}y\, \mathcal{K}(y)\delta(\Delta(y,p)) = \frac{\mathcal{K}(y_0)}{|\partial_y \Delta(y_0,p)|} \;, \tag{A.8}$$

where $y_0 > 1$ is defined through $\Delta(y_0,p) \equiv 0$, and

$$\begin{aligned}
|\partial_y\Delta_T(y_0,p)| &= -\frac{m_\mathrm{D}^2}{2}\biggl[y_0\frac{y_0^2-3}{y_0^2-1} + \frac{1}{2}\Bigl(1-y_0^2\Bigr)\ln\frac{y_0+1}{y_0-1}\biggr] \;, && \text{(A.9)}\\
|\partial_y\Delta_E(y_0,p)| &= m_\mathrm{D}^2\biggl[\frac{y_0}{y_0^2-1} - \frac{1}{2}\ln\frac{y_0+1}{y_0-1}\biggr] \;. && \text{(A.10)}
\end{aligned}$$

We note that the pole locations can be approximated as

$$y_0 \approx \left\{ \begin{array}{ll} 1 + \frac{m_\mathrm{D}^2}{4p^2} & , \quad p \gg m_\mathrm{D} \\ \frac{m_\mathrm{D}}{\sqrt{3}}\frac{1}{p} & , \quad p \ll m_\mathrm{D} \end{array} \right. \;, \quad \text{for } \Delta_T \;, \tag{A.11}$$

and

$$y_0 \approx \left\{ \begin{array}{ll} 1 + 2\exp\Bigl[-2\Bigl(\frac{p^2}{m_\mathrm{D}^2}+1\Bigr)\Bigr] & , \quad p \gg m_\mathrm{D} \\ \frac{m_\mathrm{D}}{\sqrt{3}}\frac{1}{p} & , \quad p \ll m_\mathrm{D} \end{array} \right. \;, \quad \text{for } \Delta_E \;. \tag{A.12}$$

We finally remark that the integral over the angle between $\mathbf{p}$ and $\mathbf{r}$ in Eq. (3.2) can be carried out, yielding

$$\int_{-1}^{+1} \mathrm{d}z \, \frac{2 - e^{iprz} - e^{-iprz}}{2} = 2\Big[1 - \frac{\sin(pr)}{pr}\Big] \, , \tag{A.13}$$

$$\int_{-1}^{+1} \mathrm{d}z \, \frac{2 - e^{iprz} - e^{-iprz}}{2z^2} = 2\Big[\cos(pr) - 1 + pr\,\mathrm{Si}(pr)\Big] \, , \tag{A.14}$$

where $\mathrm{Si}(z) \equiv \int_0^z \mathrm{d}t \, \sin(t)/t$. Then a two-dimensional integral is left over: the inner integration over p^0, the outer integration over p.

References

[1] T. Matsui and H. Satz, Phys. Lett. B 178 (1986) 416.

[2] H. Satz, J. Phys. G 32 (2006) R25 [hep-ph/0512217].

[3] L.D. McLerran and T. Toimela, Phys. Rev. D 31 (1985) 545; H.A. Weldon, Phys. Rev. D 42 (1990) 2384; C. Gale and J.I. Kapusta, Nucl. Phys. B 357 (1991) 65.

[4] S. Digal, P. Petreczky and H. Satz, Phys. Lett. B 514 (2001) 57 [hep-ph/0105234].

[5] C.Y. Wong, Phys. Rev. C 72 (2005) 034906 [hep-ph/0408020].

[6] F. Arleo, J. Cugnon and Y. Kalinovsky, Phys. Lett. B 614 (2005) 44 [hep-ph/0410295].

[7] M. Mannarelli and R. Rapp, Phys. Rev. C 72 (2005) 064905 [hep-ph/0505080].

[8] W.M. Alberico, A. Beraudo, A. De Pace and A. Molinari, Phys. Rev. D 72 (2005) 114011 [hep-ph/0507084]; hep-ph/0612062.

[9] A. Mócsy and P. Petreczky, Phys. Rev. D 73 (2006) 074007 [hep-ph/0512156]; arXiv:0705.2559 [hep-ph].

[10] M. Laine, O. Philipsen, P. Romatschke and M. Tassler, JHEP 03 (2007) 054 [hep-ph/0611300].

[11] F. Karsch, E. Laermann, P. Petreczky and S. Stickan, Phys. Rev. D 68 (2003) 014504 [hep-lat/0303017].

[12] G. Aarts and J.M. Martínez Resco, Nucl. Phys. B 726 (2005) 93 [hep-lat/0507004].

[13] G. Aarts and J. Foley [UKQCD Collaboration], JHEP 02 (2007) 062 [hep-lat/0612007].

[14] W.E. Caswell and G.P. Lepage, Phys. Lett. B 167 (1986) 437; N. Brambilla, A. Pineda, J. Soto and A. Vairo, Rev. Mod. Phys. 77 (2005) 1423 [hep-ph/0410047].

[15] K.G. Chetyrkin and M. Steinhauser, Phys. Rev. Lett. 83 (1999) 4001 [hep-ph/9907509].

[16] A. Czarnecki and K. Melnikov, Phys. Rev. Lett. 80 (1998) 2531 [hep-ph/9712222]; M. Beneke, A. Signer and V.A. Smirnov, Phys. Rev. Lett. 80 (1998) 2535 [hep-ph/9712302].

[17] W.H. Press, S.A. Teukolsky, W.T. Vetterling and B.P. Flannery, *Numerical Recipes in Fortran 77* (Cambridge University Press, Cambridge, 2001).

[18] K. Kajantie, M. Laine, K. Rummukainen and M. Shaposhnikov, Nucl. Phys. B 503 (1997) 357 [hep-ph/9704416].

[19] T. Umeda, K. Nomura and H. Matsufuru, Eur. Phys. J. C 39S1 (2005) 9 [hep-lat/0211003].

[20] M. Asakawa and T. Hatsuda, Phys. Rev. Lett. 92 (2004) 012001 [hep-lat/0308034].

[21] S. Datta, F. Karsch, P. Petreczky and I. Wetzorke, Phys. Rev. D 69 (2004) 094507 [hep-lat/0312037].

[22] H. Iida, T. Doi, N. Ishii, H. Suganuma and K. Tsumura, Phys. Rev. D 74 (2006) 074502 [hep-lat/0602008].

[23] G. Aarts, C.R. Allton, R. Morrin, A.P.O. Cais, M.B. Oktay, M.J. Peardon and J.I. Skullerud, PoS LAT2006 (2006) 126 [hep-lat/0610065]; G. Aarts, C.R. Allton, M.B. Oktay, M.J. Peardon and J.I. Skullerud, arXiv:0705.2198 [hep-lat].

[24] A. Jakovác, P. Petreczky, K. Petrov and A. Velytsky, Phys. Rev. D 75 (2007) 014506 [hep-lat/0611017].